



Host–guest complexes vs. supramolecular polymers in chalcogen bonding receptors: an experimental and theoretical study†

Encarnación Navarro-García,^a Bartomeu Galmés,^b José Luis Esquivel,^{ID}^a
María D. Velasco,^a Adolfo Bastida,^{ID}^c Fabiola Zapata,^{ID}^a Antonio Caballero^{ID}^{*a}
and Antonio Frontera^{ID}^{*b}

We describe here a comparative study between two tripodal anion receptors based on selenophene as the binding motif. The receptors use benzene or perfluorobenzene as a spacer. The presence of the electron-withdrawing ring activates the selenium atom for anion recognition inducing the formation of self-assembled supramolecular structures in the presence of chloride or bromide anions, which are bonded by the cooperative action of hydrogen and chalcogen bonding interactions. DOSY NMR and DLS experiments provided evidence for the formation of the supramolecular structures only in the presence of a perfluorobenzene based anion receptor while the analogous benzene one shows the classical anion/receptor complex without the participation of the selenium atom. The energetic and geometric features of the complexes of both receptors with the Cl and Br anions have been studied in solution. These results combined with the molecular electrostatic potential (MEP) surface plots allow us to rationalize the quite different behaviors of both receptors observed experimentally.

Introduction

The study of new non-covalent interactions is one of the most intense research fields within supramolecular chemistry due to the important role it plays in molecular recognition, crystal engineering and biological systems among others.¹

Without a doubt, hydrogen bonds are the most studied non-covalent interactions to date.²

In the last decade, the study of atoms that can form non-covalent interactions with electron-rich species has become a hot topic in the field of supramolecular chemistry. These new non-covalent interactions are based on the concept of σ holes introduced by Politzer and Murray, who provided a logical explanation for the formation of non-covalent interactions between halogen atoms and electron-rich species³ by the existence of a positive region in the halogen atom. The presence of one or more positive regions in determinate atoms, generally

atoms of the groups 15 to 17, is due to the anisotropy of the electron density in atoms that generates the so-called σ -hole. Obviously, this positive region (σ -hole) is associated with a negative electron density (σ -lumps).⁴ Among all of the atoms that present σ -holes, halogen atoms have been the most explored and a remarkable number of examples have been described.⁵ Analogous to hydrogen bonding interactions, these new interactions were named halogen, chalcogen, pnictogen or tetrel bonding interactions.

The term chalcogen bonding (ChB) refers to a subgroup of the σ -hole family that originates from the interactions between an electron-rich species and the σ -holes of an element belonging to group 16.⁶ To date, almost all of the investigations about chalcogen bonding have been conducted in crystal engineering,⁷ catalysis,⁸ self-assembly processes⁹ and materials design.¹⁰ Despite progress in chalcogen bonding interactions in solution,¹¹ the knowledge of this interaction in solution is still in its infancy, which is surprising given its potential similarities with halogen bonding.

In the last few years, the development of new supramolecular architectures through the self-assembly of two or more molecular components using non-covalent interactions has grown tremendously. Nowadays, the most common strategies used for the formation of supramolecular polymers are multiple hydrogen-bonding interactions,¹² hydrophobic interactions,¹³ metal–ligand coordination,¹⁴ and the combination of π – π and hydrogen-

^aDepartamento de Química Orgánica, Universidad de Murcia, Campus de Espinardo, 30100 Murcia, Spain. E-mail: antocaba@um.es

^bDepartment of Chemistry, Universitat de les Illes Balears, Crta. de Valldemossa km 7.5, 07122 Palma de Mallorca, Spain. E-mail: toni.frontera@uib.es

^cDepartamento de Química Física, Universidad de Murcia, Campus de Espinardo, 30100 Murcia, Spain

†Electronic supplementary information (ESI) available: NMR experiment, thermodynamic model, computational results. See DOI: 10.1039/d1dt03925c

bonding interactions.¹⁵ The construction of supramolecular polymers using anions as a trigger is extremely rare.

Our research group has recently reported a preference of some polydentate halogen-bonding anion receptors to form anion-induced supramolecular polymers through the anion-recognition process by a simple receptor.¹⁶

We describe here a comparative study between two tripodal chalcogen-bonding anion receptors bearing benzene or perfluorobenzene as the spacer and selenophene as the chalcogen bond donor. The presence of spacers with different electronic properties has allowed us to study the effect of their electronic nature on the formation of new anion-induced supramolecular polymers in solution. DFT calculations provided further insight into the geometric features of such supramolecular assemblies and provided an explanation for the different behaviors of both receptors.

Results and discussion

Design and synthesis

The structures of the proposed tripodal anion receptors contain two different types of aromatic rings, benzene or 2,4,6-trifluorobenzene, as spacers and three units of selenophene as the chalcogen bonding donors.

The tripodal chalcogen bonding receptors 2 and 3 were prepared *via* a Stille coupling reaction using 2-(tributylstannyl)selenophene 1¹⁷ as the starting material with 1,3,5-triiodobenzene or 1,3,5-trifluoro-2,4,6-triiodobenzene in the presence of tetrakis(triphenylphosphine)palladium catalysts (Scheme 1). Receptors 2 and 3 were obtained in moderate yields and were fully characterized using standard techniques: ¹H NMR, ¹³C NMR and FAB mass spectrometry.

Anion binding studies

The anion binding properties of chalcogen bonding receptors 2 and 3 were evaluated by ¹H NMR and ⁷⁷Se NMR spectroscopy in tetrahydrofuran-*d*₈ against the Cl⁻, Br⁻, I⁻, NO₃⁻, AcO⁻, H₂PO₄⁻ and PF₆⁻ anions added as tetrabutylammonium salts.

The ¹H NMR spectra of receptors 2 and 3 exhibit the expected signals attributed to the mono-substituted selenophene unit, two doublets of doublets corresponding to the H_a (δ = 7.99–8.34 ppm) and H_b (δ = 7.54–7.71 ppm) and one multi-

plet assigned to H_c around the δ = 7.4 ppm protons. The presence of the electron-withdrawing fluorobenzene rings causes a downfield shift in those signals regarding the analogous receptor bearing the benzene ring. In addition, receptor 2 also shows a singlet attributed to the resonance of the H_d proton of the trisubstituted benzene in the aromatic region (δ = 7.63 ppm).

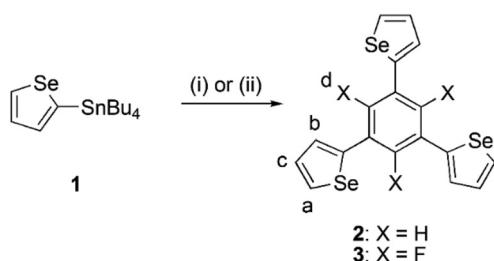
On the other hand, the ⁷⁷Se NMR spectra of receptors 2 and 3 show a singlet at δ = 595 ppm and a triplet at δ = 654 ppm, respectively.

The addition of increasing amounts of the I⁻, NO₃⁻, AcO⁻, H₂PO₄⁻ and PF₆⁻ anions to the solutions of receptors 2 and 3 (*c* = 2.5 × 10⁻³ M in tetrahydrofuran-*d*₈) did not promote significant alterations in their ¹H NMR spectra. On the contrary, the presence of the Cl⁻ or Br⁻ anions promotes a progressive down-field shift in the resonances of some of the protons. The changes observed consist of a down-field shift (Δδ = 0.11–0.06 ppm) of the signal attributed to the H_a proton closest to the Se atom in the receptors. Interestingly, the presence of the Cl⁻ and Br⁻ anions also promotes a down-field shift in the signal attributed to the proton H_b but only in the benzene-based receptor 2 (Δδ = 0.07–0.04 ppm). The different behaviours observed between receptors 2 and 3, bearing benzene or 2,4,6-trifluorobenzene rings, respectively, suggest that the anion recognition process occurs by a different binding mode. The resonances of the protons at the heterocyclic ring, H_c, and the benzene, H_d, were practically unaffected in the presence of the Cl⁻ and Br⁻ anions (Fig. 1).

In order to elucidate the role of the Se atom in the recognition process, ⁷⁷Se NMR experiments were carried out. The addition of the Cl⁻ or Br⁻ anions to a solution of receptor 2 bearing the benzene ring, did not induce remarkable changes in the peak attributed to the Se atom which clearly indicates no participation of the selenium atom in the binding event (Fig. 2a). On the contrary, in the presence of the electron-withdrawing 2,4,6-trifluorobenzene ring in the solution of receptor 3, a downfield shift was observed in the signal of the ⁷⁷Se NMR spectrum at Δδ = 0.72 ppm and Δδ = 0.98 ppm with the addition of Cl⁻ and Br⁻, respectively, which suggests participation of the Se atom in the anion binding (Fig. 2b).

The data obtained from the ¹H NMR and ⁷⁷Se NMR experiments suggest that anion binding in receptor 3, bearing the electron-withdrawing fluorobenzene group, takes place by the cooperative action of the chalcogen atom and the proton H_a of the heterocyclic ring without the participation of proton H_b while the benzene-based receptor 2 binds anions mainly by hydrogen bonding using both protons H_a and H_b.

Taking into account the results obtained from the ¹H NMR and ⁷⁷Se NMR experiments, the following binding modes are possible: (i) the non-covalent bonding of one or more anions to a single receptor using the protons H_a and/or H_b in the case of receptor 2 or (ii) through the cooperative action of proton H_a and the selenium atoms in the case of receptor 3. The formation of aggregates or supramolecular polymers in which the anions are bound through non-covalent interactions would also be possible.



Scheme 1 Synthesis of the chalcogen binding receptors 2 (i) Pd(PPh₃)₂Cl₂, 1,3,5-tribromobenzene THF and 3 (ii) 1,3,5-trifluoro-2,4,6-triiodobenzene, Pd(PPh₃)₄, and toluene.

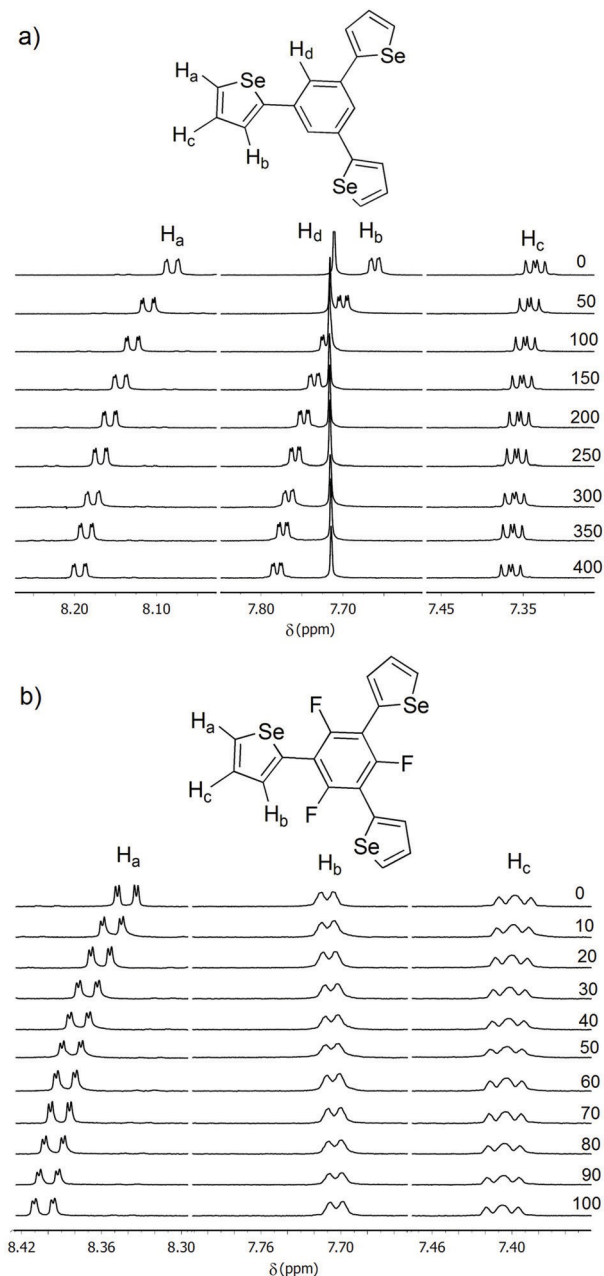


Fig. 1 Changes in the ^1H NMR spectra of receptors 2 (a) and 3 (b) ($c = 2.5 \times 10^{-3}$ M in tetrahydrofuran- d_8) with the addition of increasing amounts of Br^- anions.

In order to distinguish between the formation of supramolecular polymers or the recognition process involving a simple receptor in the solution phase, diffusion NMR experiments DOSY-NMR and dynamic light scattering (DLS) studies were carried out in tetrahydrofuran.

The formation of supramolecular polymers should cause a significant decrease in the diffusion coefficient (D) values; however, the diffusion coefficient should not be practically modified in the formation of single anion receptor complexes. The results obtained by the DOSY-NMR experiments indicate

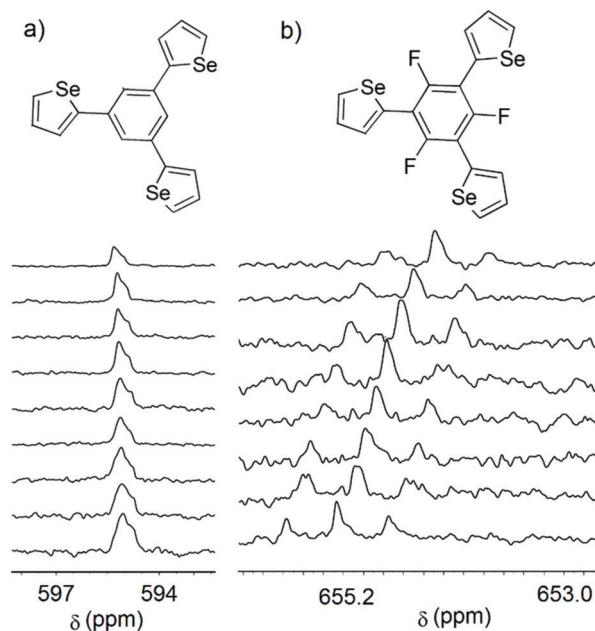


Fig. 2 Changes in the ^{77}Se NMR spectra of receptors 2 (a) and 3 (b) ($c = 0.05$ M in tetrahydrofuran- d_8) with the addition of increasing amounts of Br^- anions.

the formation of supramolecular structures when the Cl^- or Br^- anions were added to a solution of the tripodal chalcogen bonding receptor 3 ($c = 8$ mM in tetrahydrofuran- d_8). The presence of the Cl^- anions caused a significant decrease in the diffusion coefficient of receptor 3 from $D = 1.339 \times 10^{-9}$ to $0.428 \times 10^{-9} \text{ m}^2 \text{ s}^{-1}$, with $\Delta D = -68\%$. The decrease observed in the presence of the Br^- anions was also important but lower than that obtained when the Cl^- anions were added—from $D = 1.339 \times 10^{-9}$ to $0.968 \times 10^{-9} \text{ m}^2 \text{ s}^{-1}$, with $\Delta D = -28\%$. In contrast, the addition of the Cl^- or Br^- anions to a solution of receptor 2 did not modify its diffusion coefficient (Fig. 3a).

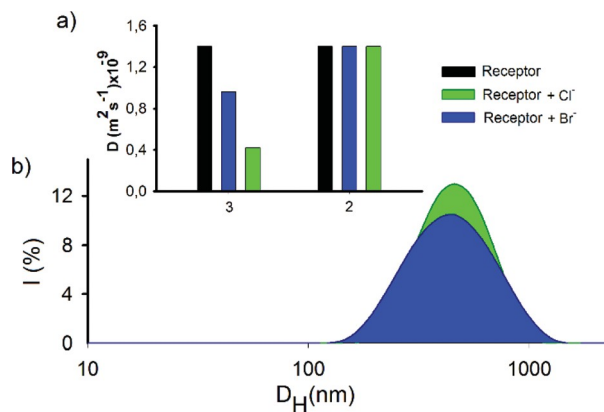
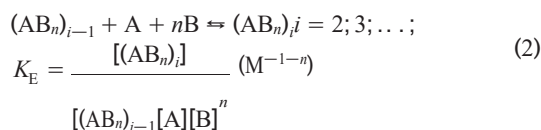
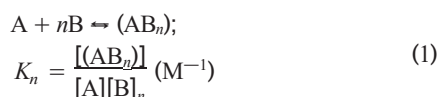


Fig. 3 (a) Changes in the diffusion coefficient (D) values of receptors 2 and 3 (black) with the addition of chloride (green) or bromide (blue) anions. (b) Distribution of the hydrodynamic diameter of receptor 3 in the presence of the chloride (green) or bromide (blue) anions.

DLS measurements at $c = 0.1$ mM in tetrahydrofuran were performed to determine the size of the supramolecular polymers. The addition of the Cl^- or Br^- anions to a solution of receptor 3 supports the formation of a large supramolecular polymer in very dilute solutions (Fig. 3b), with the values of the hydrodynamic diameters being $d_{\text{H}} = 481$ and 477 nm, respectively. In agreement with the DOSY-NMR results discussed previously, the formation of supramolecular structures in the case of receptor 2 was not observed.

Concerning the NMR shifts, the experimental values obtained for the $2 \cdot \text{Br}^-$ and $2 \cdot \text{Cl}^-$ systems are well reproduced when assuming a recognition process with a 1 : 1 stoichiometry with equilibrium constants equal to 0.75 M^{-1} and 1.1

M^{-1} , respectively. For $3 \cdot \text{Br}^-$ and $3 \cdot \text{Cl}^-$, it is necessary to model the formation of the supramolecular polymers and we have applied the methodology developed by our research group in previous works¹⁶ using a cooperative polymerization mechanism, which is characterized by two equilibrium constants corresponding to the nucleation (K_{N}) and elongation (K_{E}) steps



where A, B and $(AB)_i$ denote the receptor, the anion, and the supramolecular polymer of length i , respectively. In particular,^{16b} we have shown that not only the equilibrium constants but also the stoichiometry of the supramolecular polymer can be reasonably estimated by fitting the measured NMR shifts using the following weighted sum:

$$\delta = \frac{[A]}{C_{\text{A}}}\delta_{\text{A}} + \frac{C_{\text{A}} - [A]}{C_{\text{A}}}\delta_{\text{sp}} \quad (3)$$

where δ_{A} and δ_{sp} are the NMR shifts of the isolated receptor and the supramolecular polymer, respectively, and C_{A} is the total concentration of A. Therefore, we carried out a first set of fits, in which the n stoichiometric coefficient was also considered as a fitting parameter and provided the values 1.0 and

0.91 for the $3 \cdot \text{Br}^-$ and $3 \cdot \text{Cl}^-$ polymers, respectively, which strongly suggest a 1 : 1 stoichiometry. In the second sets of fits (see the ESI†), the value of n was fixed to 1 providing $K_{\text{N}} = 3.7 \text{ M}^{-1}$ and $K_{\text{E}} = 3.3 \times 10^{-1} \text{ M}^{-2}$ for $3 \cdot \text{Br}^-$ and $K_{\text{N}} = 3.6 \text{ M}^{-1}$ and $K_{\text{E}} = 6.4 \times 10^{-3} \text{ M}^{-2}$ for $3 \cdot \text{Cl}^-$.

The data obtained from the NMR, DOSY and DLS experiments as well as the stoichiometries obtained suggest that receptor 2 binds one Cl^- or Br^- anion forming the classical anion–receptor complex, while receptor 3 could form a supramolecular polymer.

MEP surface analysis

The MEP surfaces of receptors 2 (two conformations) and 3 are depicted in Fig. 4. It can be observed that the MEP maximum

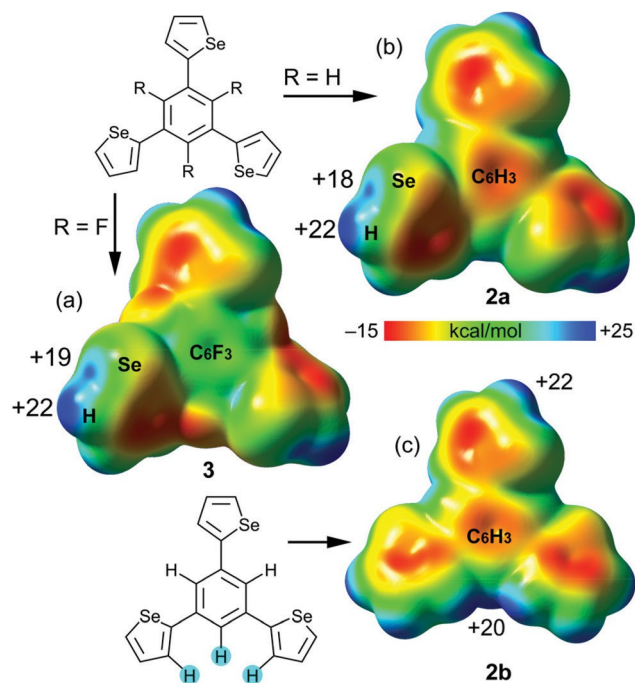


Fig. 4 MEP surfaces of receptors 2a (a), 3 (b) and 2b (c). The MEP values at selected points of the surfaces are indicated in kcal mol^{-1} .

is located for both receptors at the H_{a} protons ($+22 \text{ kcal mol}^{-1}$). The value at the Se σ -hole is slightly smaller ($+18$ for 2a and $+19$ for 3). The other Se atom σ -hole is not accessible. Moreover, in the case of 3, the hidden σ -holes interact with the nearby fluorine atoms forming intramolecular ChBs, thus reducing the intensity of the accessible σ -holes. This likely explains why the sigma holes in 2a and 3 are almost the same, although the C_6F_3 moiety should be more electron withdrawing than C_6H_3 . A similar interplay in divalent anion-binding has been reported for pnictogen-binding anion transporters and catalysts.^{8d} For receptor 2, we also studied a different conformation, where one of the selenophene rings is rotated, and is denoted as 2b in Fig. 4. This conformation is slightly more stable in THF ($0.2 \text{ kcal mol}^{-1}$) and is isoenergetic in the gas phase. The rotational barrier is very small ($2.7 \text{ kcal mol}^{-1}$ in the gas phase and $2.8 \text{ kcal mol}^{-1}$ in THF) and thus both of the rotamers likely coexist at room temperature. Rotamer 2b presents three CH bonds (two $\text{C}-\text{H}_{\text{c}}$ and one $\text{C}-\text{H}_{\text{d}}$, see Fig. 1a for the labelling of H-atoms) pointing in the same direction and thus is adequate for interacting with small anions like Cl^- and Br^- and establishing three concurrent $\text{CH}\cdots\text{X}$ interactions. The MEP value at the small cleft formed by the three C–H groups is $+20 \text{ kcal mol}^{-1}$ (see Fig. 4c), slightly smaller than the MEP value at H_{a} ($+22 \text{ kcal mol}^{-1}$) and larger than the value at the Se's σ -hole ($+18 \text{ kcal mol}^{-1}$). The formation of a similar cleft upon rotation of one selenophene ring is not possible in compound 3 due to the presence of the fluorine substituents in the central aromatic ring. For this compound, both of the rotamers are isoenergetic in the gas phase and in THF.

Geometric and energetic analyses

The geometries and binding energies of the chloride and bromide complexes with receptors 2 and 3 have been computed in this work. Those corresponding to Cl^- are discussed below (Fig. 5–7) and those of Br^- are given in the ESI (see Fig. S9 and S10†). Comparable results were obtained; the main differences are the binding energies, which are more favorable for Cl^- .

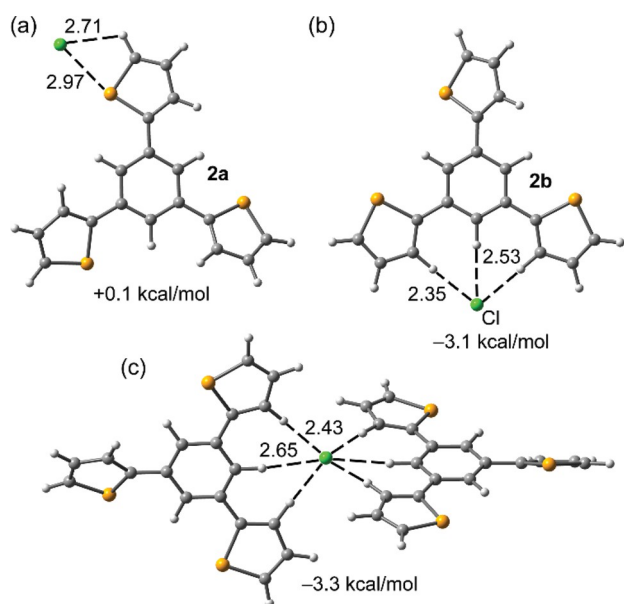


Fig. 5 PBE0-D3/def2-TZVP optimized geometries of the chloride complexes with receptor 2. Binding energies are given using THF as the solvent.

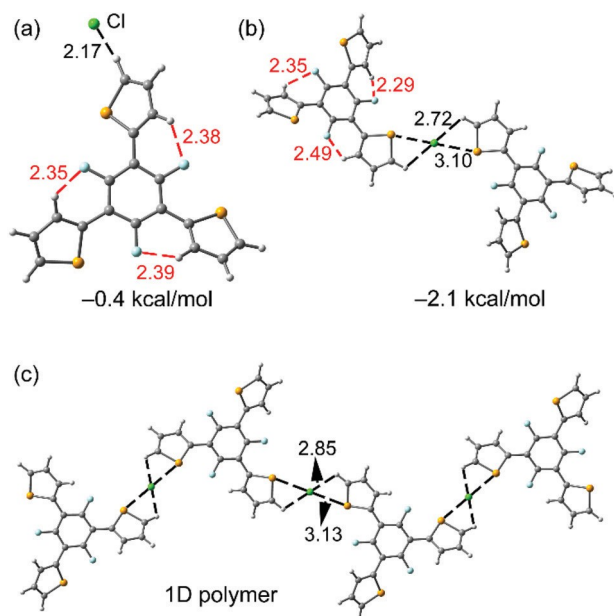


Fig. 6 PBE0-D3/def2-TZVP optimized geometries of the chloride complexes with receptor 3. Binding energies are given using THF as the solvent.

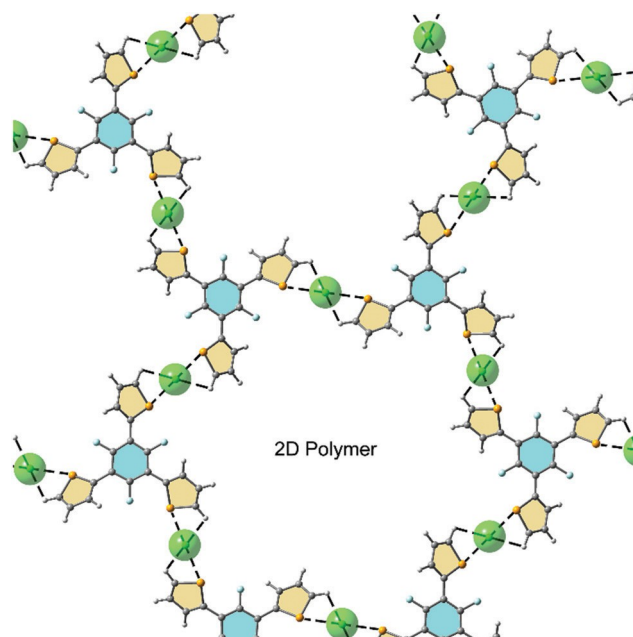


Fig. 7 Proposed 2D polymer generated by the assembly of 1D polymeric chains.

The geometries of the chloride complexes with receptors 2a and 2b are given in Fig. 5. The binding mode *via* the concurrent HB and ChB interaction is less favored ($+0.1 \text{ kcal mol}^{-1}$, see Fig. 5a) than that using the three $\text{CH}\cdots\text{Cl}^-$ interactions ($-3.1 \text{ kcal mol}^{-1}$). The $\text{C}-\text{H}_a\cdots\text{Cl}^-$ distance is longer (2.53 Å) than the $\text{C}-\text{H}_b\cdots\text{Cl}^-$ (2.35 Å) distance. This is in agreement with the chemical shift change of these protons during the titration, which is more pronounced in H_b . The fact that H_a is also affected during the titration (see Fig. 1a) can be related to the coexistence of both of the binding modes. That is, the interaction of the tripodal receptor with Cl^- *via* trifurcated H-bonds occurs through two selenophene moieties and through ChB + HB using the remaining selenophene moiety. We also studied the energetic analysis of the interaction of chloride with two receptors establishing six $\text{CH}\cdots\text{Cl}^-$ contacts (see Fig. 5c), which is also energetically favored ($-3.3 \text{ kcal mol}^{-1}$). However, the binding energy of the ternary complex is very similar to the 1 : 1 complex, thus revealing that the binding of the second receptor is not very favored. Therefore, the formation of the ternary complex is not likely to occur due to the unfavorable entropic effects, which is in line with the 1 : 1 stoichiometry observed experimentally (*vide supra*). The formation of the trifurcated H-bonding assemblies would explain the fact that receptor 2 does not form supramolecular polymers upon addition of the anion, in contrast to receptor 3. Moreover, the formation of the assembly shown in Fig. 5c would also explain the selectivity to small and monoatomic anions like Cl and Br^- over polyatomic anions or the larger iodide where the formation of six H-bonds is not possible.

A similar study has been performed for receptor 3. The geometric features of the complexes are given in Fig. 6. The chloride complex *via* a single $\text{CH}\cdots\text{Cl}^-$ bond exhibits a modest inter-

action energy ($-0.4 \text{ kcal mol}^{-1}$ in THF). The 2 : 1 complex presents a quite different binding mode, where two ChBs and two HBs are established, in line with the MEP surface analysis (see Fig. 6b) and the NMR titration experiments that show a shift in the ^{77}Se -NMR signal as well as a significant shift of H_a in the ^1H -NMR spectra (see Fig. 1 and 2). The interaction energy is favorable ($-2.1 \text{ kcal mol}^{-1}$), though less favorable than the 1 : 1 complex of receptor 2 (Fig. 5b).

The examination of the optimized geometries reveals the formation of the intramolecular $\text{C}-\text{H}_b\cdots\text{F}$ interactions (see red dashed lines in Fig. 6a and b) that likely explain the change in the H_b signal during the titrations (see Fig. 1b) as the complexation of 3 with the Cl^- anion affects the geometry and strength of the intramolecular H-bonds.

Fig. 6c shows an optimized 4 : 3 complex as the model of the supramolecular 1D polymer that propagates *via* the formation of two $\text{Se}\cdots\text{Cl}^-$ and two $\text{CH}\cdots\text{Cl}^-$ interactions with the selenophene rings of two adjacent receptors. Such 1D polymers could aggregate forming 2D polymers like those shown in Fig. 7 where each selenophene interacts with one chloride anion forming 2D supramolecular assemblies with large void spaces. These can be occupied by solvent molecules and counterions, providing solubility. Such assemblies are also feasible for compound 2; however, its interaction with Cl^- *via* trifurcated H-bonds is energetically favored with respect to the ChB and HBs. This likely explains the different behaviors observed in both compounds regarding the formation of supramolecular polymers or 1 : 1 complexes.

Finally, it should be emphasized that the intention of this theoretical study is not to provide accurate binding energies, which can be obtained directly from the experimental equilibrium/nucleation constants. Instead, it is to provide a plausible explanation for the experimental findings regarding the different behaviours of both receptors. The small equilibrium (or nucleation) constants observed experimentally ($K \approx 1 \text{ M}^{-1}$ for 2 \cdots halide and $K_N \approx 3.6 \text{ M}^{-1}$ for 3 \cdots halide) agree with the fact that the binding energies are very small as are those obtained theoretically. In fact, the free energy (ΔG) is around zero for 2 interacting with chloride ($K = 1.1$) and even positive for bromide ($K = 0.75$), which agrees well with the great excess of anions needed in the titrations (up to 400 equivalents in 2). It should be also stressed that the entropic effects are not well reproduced by computational methods in complicated host-guest systems and polymers. In addition, the solvent effects considered here use a continuum model, another approximation to the real experimental conditions. Finally, the counterion effects are also not considered. Bearing in mind the limitations of this theoretical study, our intention here is to rationalize the experimental findings and to provide some plausible geometries that agree with the NMR data instead of providing highly accurate binding energies.

Experimental section

All of the reactions were carried out using solvents that were dried by routine procedures. All of the melting points were

determined by means of a Kofler hot-plate melting-point apparatus and are uncorrected. ^1H , ^{13}C and ^{77}Se NMR spectra were recorded in solution using a Bruker 300, 400, or 600 MHz spectrometer. The following abbreviations have been used to state the multiplicity of the signals: s (singlet), m (multiplet), dd (doublet of doublets), dm (doublet of multiplets), td (triplet of doublets) and q (quaternary carbon). Chemical shifts (δ) in the ^1H and ^{13}C NMR spectra are referenced to tetramethylsilane (TMS). Diffusion NMR experiments (DOSY) were recorded using a Bruker 600 spectrometer (^1H) using the LED-BPP sequence with a diffusion period (Δ) of 150 ms, field gradient pulses (δ) of 4 ms were applied as half-sine profile bipolar pairs and an LED period of 5 ms. The field gradients were varied from 2–90% of maximum (53 G cm^{-1}) in 16 steps and data were analysed using the Bruker TOPSPIN 2.1 software. Mass spectra were recorded using a Fisons AUTOSPEC 500 VG spectrometer and the FAB+ mass spectra were recorded with 3-nitrobenzyl alcohol as a matrix. Dynamic light scattering analyses were performed using a Malvern Zetasizer Nano ZS (Malvern Instruments Ltd, UK) at 25°C with a 173° angle relative to the source. The hydrodynamic diameter distributions were obtained by volume using the software package of the apparatus. Each curve represents the average of 3 measurements (16 runs each). Prior to analysis, all of the solutions were filtered.

Synthesis of 1,3,5-tri(selenophen-2-yl)benzene (2)

To a stirred solution of tributyl(selenophen-2-yl)stannane 1 (1.26 g, 3.00 mmol) and 1,3,5-tribromobenzene (0.12 g, 0.37 mmol) in dry THF (10 mL), $\text{Pd}(\text{PPh}_3)_2\text{Cl}_2$ (24 mg, 0.037 mmol) was added. The reaction mixture was stirred under N_2 for 18 h at 60°C . The solvent was removed and the resulting residue was purified by silica gel column chromatography (hexane/ CH_2Cl_2 5 : 1) to give a yellow solid. Yield: 48.0%; mp: $139\text{--}140^\circ\text{C}$; ^1H NMR (400 MHz, tetrahydrofuran- d_8): δ 8.08 (3H, dd, $J = 5.6 \text{ Hz}$, $J = 1.1 \text{ Hz}$), 7.71 (3H, s), 7.66 (3H, dd, $J = 3.8 \text{ Hz}$, $J = 1.1 \text{ Hz}$), 7.33 (3H, dd, $J = 5.6 \text{ Hz}$, $J = 3.8 \text{ Hz}$) ppm; ^{13}C NMR (100 MHz, CDCl_3): δ 150.7, 138.7, 131.8, 131.6, 127.1, 124.7 ppm; MS (GC): m/z calc. for $[\text{M} + \text{H}]^+$ 466.8, found 466.8.

Synthesis of 1,3,5-tri(selenophen-2-yl)perfluorobenzene (3)

To a stirred solution of tributyl(selenophen-2-yl)stannane 1 (1.73 g, 4.12 mmol) and 1,3,5-trifluoro-2,4,6-triiodobenzene (0.5 g, 0.98 mmol) in dry toluene (10 mL), $\text{Pd}(\text{PPh}_3)_4$ (0.23 g, 0.20 mmol) was added. The reaction mixture was stirred under N_2 for 72 h at 110°C . The solvent was removed and the resulting residue was purified by silica gel column chromatography using hexane to give a white solid. Yield: 18.0%; decompose: 210°C ; ^1H NMR (300 MHz, tetrahydrofuran- d_8): δ 8.34 (3H, dd, $J = 5.7 \text{ Hz}$, $J = 1.0 \text{ Hz}$), 7.71 (3H, dd, $J = 3.9 \text{ Hz}$), 7.41–7.39 (3H, m) ppm; ^{13}C NMR (75 MHz, CDCl_3): δ 155.1 (dt, $J = 252 \text{ Hz}$, $J = 9.2 \text{ Hz}$), 134.1, 133.4, 133.1, 130.5, 112.5 (t, $J = 11.8 \text{ Hz}$) ppm; MS (GC): m/z calc. for $[\text{M} + \text{H}]^+$ 519.9, found 519.9.

Theoretical methods

The energies of all of the complexes included in this study were computed at the PBE0-D3/def2-TZVP level of theory. The

geometries have been fully optimized by using the program TURBOMOLE.¹⁸ The interaction energy (or binding energy in this work), ΔE , is defined as the energy difference between the optimized complex and the sum of the energies of the optimized monomers. For the calculations, we have used the Weigend def2-TZVP¹⁹ basis set and the PBE0²⁰ DFT functional. The MEP (Molecular Electrostatic Potential) surface calculations were computed using the Gaussian-16 software at the PBE1PBE-D3/def2-TZVP level of theory.²¹ PBE1PBE is the notation used by Gaussian-16 for the hybrid functional PBE0. The solvent effects (THF) were taken into account by using the PCM continuum model.²²

Conclusions

We show here the different behaviors of two structurally analogous anion receptors. The activation of the sigma holes on the selenium atom by the incorporation of an electron-withdrawing ring greatly affects the anion binding mode. DOSY NMR and DLS experiments indicate a significant decrease in the diffusion coefficient of the anion complexes compared with that of the free receptor and the formation of large supramolecular structures only in the chalcogen bonding receptor 3. In contrast, the receptor bearing benzene as a spacer (2) binds the chloride and bromide anions by hydrogen bonding interactions without the participation of the selenium atom. Interestingly, no supramolecular polymers were detected in the hydrogen bonding anion receptor. DFT calculations explain the different behaviors observed in both of the compounds regarding the formation of supramolecular polymers. The future direction of this work will involve the utilization of oxyanions and the removal of one selenophene in 3 to construct supramolecular macrocycles.

Conflicts of interest

There are no conflicts to declare.

Acknowledgements

We thank the MICIU/AEI (projects CTQ2017-86775-P, CTQ2016-79345P, PID2020-113483GB-I00, PID2020-115637GB-I00 and RED2018-102331-T FEDER funds) and the Fundación Séneca Región de Murcia (CARM) (projects 20819/PI/18 and 20789/PI/18) for financial support. We thank the CTI (UIB) for the use of their computational facilities.

Notes and references

- (a) S. Scheiner, *Hydrogen Bonding A Theoretical Perspective*, Oxford University Press, New York, 1997; (b) Y. Feng, D. Rainteau, C. Chachaty, Z. W. Yu, C. Wolf and P. J. Quinn, *Biophys. J.*, 2004, 86, 2208–2217; (c) F. G. Wu,

- N. N. Wang and Z. W. Yu, *Langmuir*, 2009, 25, 13394–13401.
- (a) H. J. Schneider, *Angew. Chem., Int. Ed.*, 2009, 48, 3924–3977; (b) J. M. Lehn, *Supramolecular chemistry concepts and perspectives*, Wiley-VCH, Weinheim, 1995; (c) J. W. Steed and J. L. Atwood, *Supramolecular chemistry*, Wiley, Chichester, 2000; (d) G. Gilli and P. Gilli, *The Nature of the Hydrogen Bond*, Oxford University Press, Oxford, 2009; (e) G. R. Desiraju and T. Steiner, *The Weak Hydrogen Bond in Structural Chemistry and Biology*, Oxford, New York, 1999; (f) S. Scheiner, *Hydrogen Bonding. A Theoretical Perspective*, Oxford University Press, New York, 1997; (g) S. J. Grabowski, *Hydrogen Bonding—New Insights*, Springer, Amsterdam, 2006; (h) I. Alkorta, J. Elguero and A. Frontera, *Crystals*, 2020, 10, 180.
- P. Politzer, J. S. Murray and T. Clark, *Phys. Chem. Chem. Phys.*, 2010, 12, 7748.
- (a) P. Politzer and J. S. Murray, *Crystals*, 2017, 7, 212–226; (b) J. S. Murray, P. Lane, T. Clark, K. E. Riley and P. Politzer, *J. Mol. Model.*, 2012, 18, 541–548.
- (a) G. Cavallo, P. Metrangolo, R. Milani, T. Pilati, A. Primagi, G. Resnati and G. Terraneo, *Chem. Rev.*, 2016, 116, 2478; (b) L. C. Gilday, S. W. Robinson, T. A. Barendt, M. J. Langton, B. R. Mullaney and P. D. Beer, *Chem. Rev.*, 2015, 115, 7118; (c) L. González, F. Zapata, A. Caballero, P. Molina, C. Ramírez de Arellano, I. Alkorta and J. Elguero, *Chem. – Eur. J.*, 2016, 22, 7533; (d) F. Zapata, S. J. Benítez-Benítez, P. Sabater, A. Caballero and P. Molina, *Molecules*, 2017, 22, 2273; (e) P. Sabater, F. Zapata, A. Caballero, N. de la Visitación, I. Alkorta, J. Elguero and P. Molina, *J. Org. Chem.*, 2016, 81, 744; (f) F. Zapata, A. Caballero and P. Molina, *Eur. J. Inorg. Chem.*, 2017, 237; (g) D. F. Mertsalov, R. M. Gomila, V. P. Zaytsev, M. S. Grigoriev, E. V. Nikitina, F. I. Zubkov and A. Frontera, *Crystals*, 2021, 11, 1406.
- (a) A. Bauzá, T. J. Mooibroek and A. Frontera, *ChemPhysChem*, 2015, 16, 2496–2517; (b) D. J. Pascoe, K. B. Ling and S. L. Cockroft, *J. Am. Chem. Soc.*, 2017, 139, 15160–15167; (c) S. Scheiner, *Chem. – Eur. J.*, 2016, 22, 18850–18858; (d) J. Y. C. Lim and P. D. Beer, *Chem*, 2018, 4, 731–783.
- (a) J. Fanfrlk, A. Prda, Z. Padelkov, A. Pecina, J. Machcek, M. Lepsk, J. Holub, A. Ruzicka, D. Hnyk and P. Hobza, *Angew. Chem., Int. Ed.*, 2014, 53, 10139–10142; (b) Y. Zhang and W. Wang, *Crystals*, 2018, 8, 163; (c) R. M. Gomila and A. Frontera, *J. Organomet. Chem.*, 2021, 954–955, 122092.
- (a) S. Benz, J. López-Andarias, J. Mareda, N. Sakai and S. Matile, *Angew. Chem., Int. Ed.*, 2017, 56, 812–815; (b) S. Benz, J. Mareda, C. Besnard, N. Sakai and S. Matile, *Chem. Sci.*, 2017, 8, 8164–8169; (c) P. Wönnner, L. Vogel, M. Deser, L. Gomes, F. Kniep, B. Mallick, D. B. Werz and S. M. Huber, *Angew. Chem., Int. Ed.*, 2017, 56, 12009–12012; (d) H. V. Humeniuk, A. Gini, X. Hao, F. Coelho, N. Sakai and S. Matile, *JACS Au*, 2021, 1, 1588–1593; (e) A. Frontera and A. Bauza, *Int. J. Mol. Sci.*, 2021, 22, 12550; (f) H. S. Biswal, A. K. Sahu, B. Galmés, A. Frontera and

- D. Chopra, *ChemBioChem*, 2021, 22, DOI: 10.1002/cbic.202100498.
- 9 (a) P. C. Ho, P. Szydlowski, J. Sinclair, P. J. W. Elder, J. Keibel, C. Gendy, L. M. Lee, H. Jenkins, J. F. Britten, D. R. Morim and I. Vargas-Baca, *Nat. Commun.*, 2016, 7, 11299; (b) L. Chen, J. Xiang, Y. Zhao and Q. Yan, *J. Am. Chem. Soc.*, 2018, 140, 7079–7082.
- 10 (a) K. T. Mahmudov, M. N. Kopylovich, M. F. C. Guedes da Silva and A. J. L. Pombeiro, *Dalton Trans.*, 2017, 46, 10121–10138; (b) M. N. Piña, A. Frontera and A. Bauza, *ACS Chem. Biol.*, 2021, 16, 1701–1708; (c) J. A. Fernandez-Riveras, A. Frontera and A. Bauza, *Phys. Chem. Chem. Phys.*, 2021, 23, 17656–17662.
- 11 (a) N. A. Semenov, A. V. Lonchakov, N. A. Kushkarevsky, E. A. Suturina, V. V. Korolev, E. Lork, V. G. Vasiliev, S. N. Konchenko, J. Beckmann, N. P. Gritsan and A. V. Zibarev, *Organometallics*, 2014, 33, 4302–4314; (b) G. E. Garrett, G. L. Gibson, R. N. Straus, D. S. Seferos and M. S. Taylor, *J. Am. Chem. Soc.*, 2015, 137, 4126–4133; (c) V. Kumar, C. Leroy and D. L. Bryce, *CrystEngComm*, 2018, 20, 6406–6411; (d) G. E. Garrett, E. I. Carrera, D. S. Seferos and M. S. Taylor, *Chem. Commun.*, 2016, 52, 9881; (e) J. Y. C. Lim, I. Marques, A. L. Thompson, K. E. Christensen, V. Felix and P. D. Beer, *J. Am. Chem. Soc.*, 2017, 139, 3122–3133; (f) E. Navarro-García, B. Galmés, M. D. Velasco, A. Frontera and A. Caballero, *Chem. – Eur. J.*, 2020, 26, 4706–4713.
- 12 E. M. Todd and S. C. Zimmerman, *J. Am. Chem. Soc.*, 2007, 129, 14534–14535.
- 13 (a) A. Ustinov, H. Weissman, E. Shirman, I. Pinkas, X. Zuo and B. Rybtchinski, *J. Am. Chem. Soc.*, 2011, 133, 16201–16211; (b) S. Fujii and J. M. Lehn, *Angew. Chem., Int. Ed.*, 2009, 48, 7635–7638; (c) I. Danila, F. Riobe, F. Piron, J. Puigmarti-Luis, J. D. Wallis, M. Linares, H. Agren, D. Beljonne, D. B. Amabilino and N. Avarvari, *J. Am. Chem. Soc.*, 2011, 133, 8344–8353; (d) C. C. Lee, C. Grenier, E. W. Meijer and A. P. H. J. Schenning, *Chem. Soc. Rev.*, 2009, 38, 671–683.
- 14 (a) G. R. Whittell, M. D. Hager, U. S. Schubert and I. Manners, *Nat. Mater.*, 2011, 10, 176–188; (b) C. F. Chow, S. Fujii and J. M. Lehn, *Angew. Chem., Int. Ed.*, 2007, 46, 5007–5010; (c) W. C. Yount, D. M. Loveless and S. L. Craig, *J. Am. Chem. Soc.*, 2005, 127, 14488–14496; (d) G. Schwarz, Y. Bodenthin, Z. Tomkowicz, W. Haase, T. Geue, J. Kohlbrecher, U. Pietsch and D. G. Kurth, *J. Am. Chem. Soc.*, 2011, 133, 547–558; (e) F. S. Han, M. Higuchi and D. G. Kurth, *J. Am. Chem. Soc.*, 2008, 130, 2073–2081.
- 15 J. S. Park, K. Y. Yoon, D. S. Kim, V. M. Lynch, C. W. Bielawski, K. P. Johnston and J. L. Sessler, *Proc. Natl. Acad. Sci. U. S. A.*, 2011, 108, 20913–20917.
- 16 (a) F. Zapata, L. Gonzalez, A. Caballero, D. Bautista, A. Bastida and P. Molina, *J. Am. Chem. Soc.*, 2018, 140, 2041–2045; (b) F. Zapata, L. Gonzalez, A. Bastida, D. Bautista and A. Caballero, *Chem. Commun.*, 2020, 56, 7084–7087; (c) P. Sabater, F. Zapata, A. Bastida and A. Caballero, *Org. Biomol. Chem.*, 2020, 18, 3858–3866.
- 17 J. H. Kim, J. B. Park, S. A. Shin, M. H. Hyun and D. H. Hwang, *Polymer*, 2014, 55, 3605–3613.
- 18 R. Ahlrichs, M. Bär, M. Hacer, H. Horn and C. Kömel, *Chem. Phys. Lett.*, 1989, 162, 165–169.
- 19 (a) F. Weigend and R. Ahlrichs, *Phys. Chem. Chem. Phys.*, 2005, 7, 3297–3305; (b) F. Weigend, *Phys. Chem. Chem. Phys.*, 2006, 8, 1057–1065.
- 20 C. Adamo and V. Barone, *J. Chem. Phys.*, 1999, 110, 6158–6169.
- 21 M. J. Frisch, G. W. Trucks, H. B. Schlegel, G. E. Scuseria, M. A. Robb, J. R. Cheeseman, G. Scalmani, V. Barone, G. A. Petersson, H. Nakatsuji, X. Li, M. Caricato, A. V. Marenich, J. Bloino, B. G. Janesko, R. Gomperts, B. Mennucci, H. P. Hratchian, J. V. Ortiz, A. F. Izmaylov, J. L. Sonnenberg, D. Williams-Young, F. Ding, F. Lipparini, F. Egidi, J. Goings, B. Peng, A. Petrone, T. Henderson, D. Ranasinghe, V. G. Zakrzewski, J. Gao, N. Rega, G. Zheng, W. Liang, M. Hada, M. Ehara, K. Toyota, R. Fukuda, J. Hasegawa, M. Ishida, T. Nakajima, Y. Honda, O. Kitao, H. Nakai, T. Vreven, K. Throssell, J. A. Montgomery Jr., J. E. Peralta, F. Ogliaro, M. J. Bearpark, J. J. Heyd, E. N. Brothers, K. N. Kudin, V. N. Staroverov, T. A. Keith, R. Kobayashi, J. Normand, K. Raghavachari, A. P. Rendell, J. C. Burant, S. S. Iyengar, J. Tomasi, M. Cossi, J. M. Millam, M. Klene, C. Adamo, R. Cammi, J. W. Ochterski, R. L. Martin, K. Morokuma, O. Farkas, J. B. Foresman and D. J. Fox, *Gaussian 16, Revision C.01*, Gaussian, Inc., Wallingford CT, 2016.
- 22 J. Tomasi, B. Mennucci and R. Cammi, *Chem. Rev.*, 2005, 105, 2999–3093.